

# RELATIONSHIPS BETWEEN SEA SURFACE TEMPERATURES AND STREAMFLOWS ACROSS THE CORDILLERA DE LOS ANDES

Eduardo A. FLAMENCO<sup>1</sup>, Ricardo VILLALBA<sup>2</sup>

Instituto Nacional de Tecnología Agropecuaria, Buenos Aires, Argentina

Departamento de Dendrocronología e Historia Ambiental, IANIGLA, CONICET, Mendoza, Argentina

## 1. INTRODUCTION

Variations in ocean circulation markedly affect atmospheric conditions in the adjacent marine regions and in the surrounding lands. These changes in the ocean-atmosphere conditions can, in turn, alter the patterns of atmospheric circulation at hemispheric scale, creating a series of anomalies at global scale through teleconnections. Some modes of ocean-atmosphere variability, such as ENSO (El Niño/Southern Oscillation), NAO (North Atlantic Oscillation) and PDO (Pacific Decadal Oscillation), are associated with environmental changes in different regions of our planet. Previous studies in Argentina showed that variations in the spatial patterns of sea surface temperatures (SSTs) affected precipitation fields, and indirectly, the discharge of the Paraná and Uruguay rivers (Mechoso e Iribarren, 1992; Valdés et al., 1999; Berri et al. 1997).

The major goal of this study is to describe the relationships between interannual variations in river discharges along the Andes Cordillera and SST. Basins with different fed-precipitation regimes were selected in order to include streamflow originates from rain (Bermejo river), snowmelt (Atuel river), or a combination of both (Neuquén, Limay and Chubut rivers).

The ocean-atmosphere modes of variability previously mentioned are directly linked to the temporal-spatial evolution of the SSTs and sea level pressure on the adjacent regions. Consequently, in this study we use SSTs as an expression of these modes of variability.

## 2. MATERIALS AND METHODOLOGY

### 2.1 Spatial patterns

Monthly streamflow data were provided by the Subsecretaría de Recursos Hídricos, Argentina. The main characteristics of the selected rivers are presented in Table 1. Gridded (on 1° lat. x 1° long.) SSTs for the period 1950 – 2004 were obtained from the Climate Diagnostic Center of the National Ocean and Atmospheric Administration (Reynolds & Smith, 1994).

Oceanic regions were SSTs were statistically linked (or teleconnected) with the temporal variability of the annual mean streamflow ( $Q_{ma}$ ) of the rivers listed in Table 1 were identified. Patterns of spatial correlations between streamflows and SSTs were calculated using the CLIMLAB program (Tanco y Berri, 2000) developed at the International Research Institute (IRI) of the Lamont-Doherty Earth Observatory, University of Columbia (USA). CLIMLAB produces isoline maps connecting SST grids with equal correlation values resulting of comparing streamflows and SSTs.

| River   | Gage Station | Basin Area (km <sup>2</sup> ) | Annual Average Discharge (m <sup>3</sup> /s) | Data Period |
|---------|--------------|-------------------------------|--|-------------|
| Bermejo | Sarmiento    | 25.000                        | 354,0  | 1940-99     |
| Atuel   | Angostura    | 3.800                         | 34,8   | 1906-99     |
| Neuquén | P. Indios    | 30.843                        | 308,1  | 1903-99     |
| Limay   | Confluencia  | 26.688                        | 681,1  | 1943-99     |
| Chubut  | Altares      | 16.400                        | 46,4   | 1943-99     |

Table 1. Gauging stations and characteristics of the analyzed rivers.

### 2.2 Statistical analysis

In order to establish the statistical significance of the relationships between streamflow and SST, the degrees of freedom in the correlation analyses were adjusted taking into account the autocorrelations in the temporal series. In the process of estimating the statistical significance of the correlation coefficients, the actual number of observations was replaced by the effective number observations ( $N_{eff}$ ).  $N_{eff}$  is calculated as follows (modified from Slonosky et al., 2000).

$$N_{eff} = N \times (1 - |r_1 r_2|) / (1 + |r_1 r_2|)$$

Where  $N$  is the total number of observations and,  $r_1$  and  $r_2$  are the lag-one serial correlation coefficients of the two time series under consideration ( $Q_{ma}$  and SST). The original equation in Slonosky did not use the absolute value of the correlation product ( $r_1 r_2$ ). If such product is negative, Slonosky et al (2000) equation might produce values of  $N_{eff}$  larger than  $N$ .

To determine if the correlation coefficients between discharges and SST are statistically significant we have applied a test based on the distribution of Student.

<sup>1</sup> Instituto Nacional de Tecnología Agropecuaria  
Instituto de Clima y Agua  
Las Cabañas y Los Reseros S/N  
1712 - Castelar, Buenos Aires, Argentina.  
[lclima@inta.gov.ar](mailto:lclima@inta.gov.ar)

<sup>2</sup> Departamento de Dendrocronología e Historia Ambiental, IANIGLA, CONICET, Mendoza, Argentina

Standard Error of  $r = \sqrt{(1-r^2)/(Neff-2)}$

If the  $r$  calculated is greater than the tabulated value, which results from multiply the standard error by the  $t$ -Student with  $Neff-2$  degrees of freedom, the correlation coefficient is significant.

The Mann-Whitney test of mean population differences was applied to check temporal changes in streamflow across the Andes as well as for SSTs. River and SST time series were split in two 25-year subperiods 1950-1974 and 1975-1999 periods. For the Patagonian rivers (Limay and Chubut), a visual inspection of the records indicates a marked change in streamflows after 1983. In consequence, for the Patagonian rivers the subperiods 1950-1982 and 1983-1999 were considered.

### 3. RESULTS

#### 3.1 Spatial patterns

Figures 1 to 5 show the spatial correlation patterns between  $Qma$  and SST for those sectors of oceans where correlations are particularly significant. The  $Qma$  was calculated taken into account the hydrologic cycle of each river. For the Bermejo river the hydrologic cycle goes from September to August, for the Atuel river from July to June, and for the Neuquén, Limay and Chubut rivers from April to March.

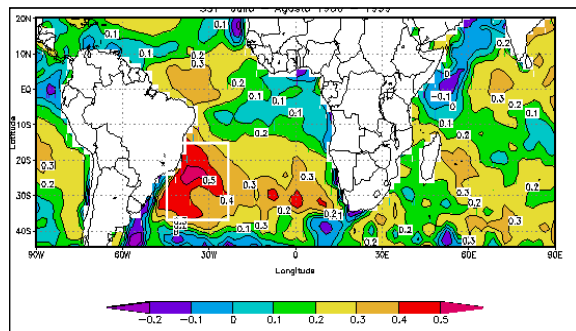


Figure 1.1 Spatial correlation pattern between the  $Qma$  from the Bermejo river and July-August SSTs for the interval 1950-1999. The white rectangle represents the area over the sea more strongly correlated with the streamflow.

In all figures, positive correlation coefficients between the  $Qma$  and SST indicate that positive departures in SSTs are related to above long-term mean streamflows. Conversely, negative correlation coefficients suggest that abundant discharges occur in conjunction with negative departures in SSTs.

The Figure 1.1 shows the spatial correlation pattern between the  $Qma$  from the Bermejo river and July-August SST during the period 1950-1999. The region located in the South Atlantic Ocean off the coast of South America between 16° and 36° S is significant correlated with the  $Qma$  from the Bermejo

river. For the sector located between 20° and 25° S,  $r$  reaches values above 0.5. During November-December, the region of highest correlations indicated in Figure 1.2 maintains correlation values superior to 0.3, however, the ocean sector more strongly correlated with the streamflow appears now above the Indian Ocean adjacent to South Africa. This region presents correlation values in the order of  $r = 0.55$ .

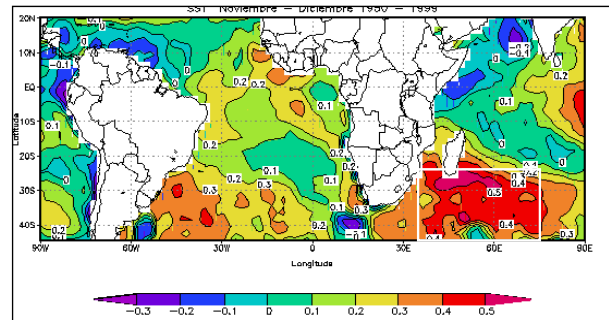


Figure 1.2 Spatial correlation pattern between the  $Qma$  from the Bermejo river and November-December SSTs during the interval 1950-1999.

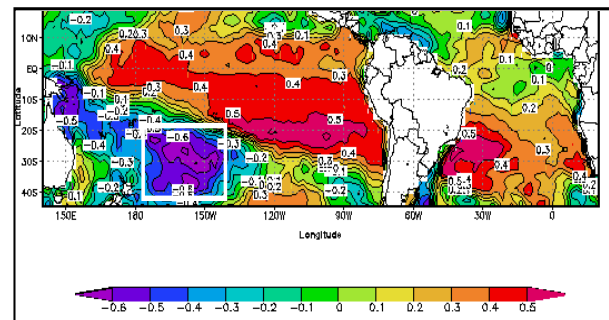


Figure 2.1 Spatial correlation pattern between the  $Qma$  from the Atuel river and July-August SSTs for the interval 1950-1999. The are on the Pacific next to the Australian coast (22° and 40° S), presents correlations with the Atuel streamflow in the order of  $r = 0.7$ .

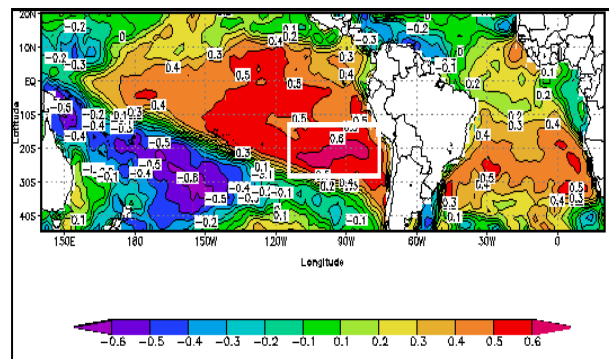


Figure 2.2 Spatial correlation pattern between the  $Qma$  from the Atuel river and September-October SSTs for the interval 1950-1999. The Pacific area off to the South American coast (10°-30° S), presents correlations in the order of  $r = 0.6$ .

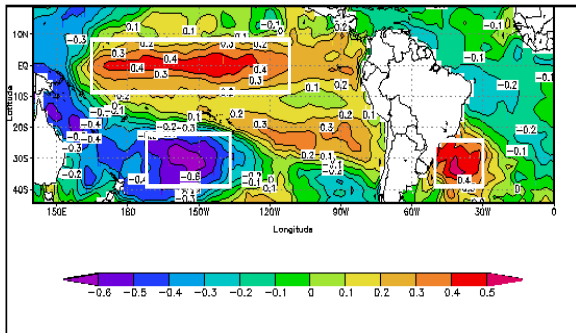


Figure 3 Spatial correlation pattern between the *Qma* from the Neuquén river and June-July SSTs during the period 1950 – 1999. White boxes delimit the areas on the sea more strongly correlated with the streamflow. The three oceanic regions strongly related to the Neuquén river streamflow are the tropical Pacific and the western subtropical Pacific in a positive way, and the western Subtropical Pacific in a negative way.

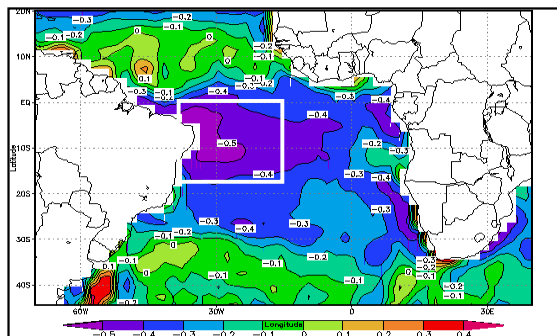


Figure 4.1 Spatial correlation pattern between the *Qma* from the Limay river and January-February SSTs during the interval 1950-1999. Correlation coefficients is in the order of  $r = -0.5$  are recorded in the area of the Atlantic Ocean in front of the NE Brazilian between  $0^\circ$  and  $20^\circ$  S.

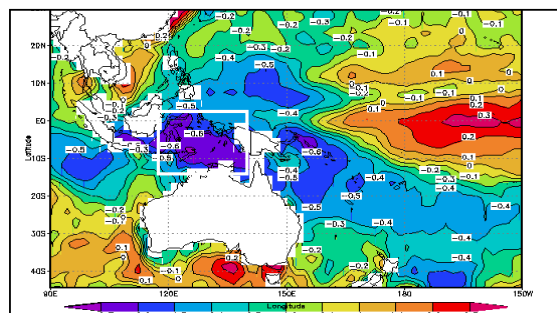


Figure 4.2 Spatial correlation pattern between the *Qma* from the Limay river and October-November SSTs during the interval 1950-1999. The region located in the west Pacific to the north of Australian reaches correlation coefficients about  $r = -0.7$ .

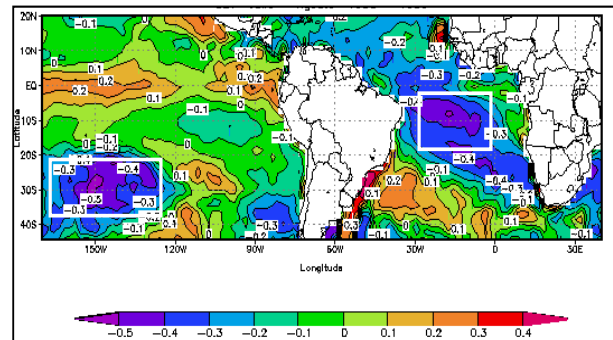


Figure 5. Spatial correlation patterns between the *Qma* from the Chubut river and July-August SSTs during the period 1950-1999. The regions located on the southwestern Pacific Ocean ( $20^\circ - 40^\circ$  S) and in the tropical Atlantic ( $0^\circ - 20^\circ$  S) are significant correlated with the Chubut river streamflow ( $r = -0.5$  and  $r = -0.4$ , respectively).

Figures 2.1 and 2.2 show the spatial correlation patterns between the annual discharges of the Atuel river and SSTs for July-August and September-October, respectively. In both patterns the east and southwest regions of the Tropical-Subtropical Pacific Ocean between  $10^\circ - 30^\circ$  S and  $22^\circ - 40^\circ$  S appear strongly correlated with the Actual river streamflow. Correlation coefficients reach absolute values between  $r = 0.6$  and  $0.7$ .

Figure 3 represents the spatial correlation pattern between the Neuquén river streamflow and June-July SSTs. Correlation values are in the order of  $r = -0.6$  in the South Pacific east of the Australian coast,  $r = 0.5$  in the South Atlantic sector close to Santa Catarina (Brazil), and  $r = 0.4$  in the Tropical Pacific.

Figures 4.1 and 4.2 represent the spatial correlation patterns between the *Qma* from the Limay river and January-February, October-November SSTs, respectively. For January-February, SSTs in the tropical Atlantic off the Brazilian coast show correlation coefficients around  $r = -0.5$ , whereas values close to  $r = -0.7$  are recorded for the western Pacific region during October and November.

Finally, the Figure 5 shows the spatial correlation patterns between the *Qma* from the Chubut river and SST across the Pacific and Atlantic Oceans. Two oceanic regions located in the Subtropical Pacific between the  $20^\circ$  and  $45^\circ$  S and in the Tropical Atlantic between  $0^\circ - 20^\circ$  S, are inversely correlated with the Chubut river streamflow.

### 3.2 Statistical analysis

Table 2 lists the correlation coefficients between the *Qma* from the five selected rivers and SSTs from the areas indicated with white rectangles in Figures 1 to 5. Correlation coefficients between streamflow and SST are indicated as calculated  $r_c$ , while the critical correlation value based on  $N_{eff}$  is designed as tabulated  $r_t$ . For all comparisons, the calculated  $r_c$  is higher than the tabulated  $r_t$ . The level of significance provides a measurement of the strength of the relationships.

For most of the analyzed rivers the Mann-Whitney test indicates that means for the selected sub-periods are significantly different, with an increase in mean discharge

during the period 1975-1999 in the basins of the Bermejo (highly significant) and Atuel (statistically significant) rivers, whereas a reduction was recorded for the Limay and Chubut rivers. There are no significant changes in the Neuquén river between these periods (Table 3).

Significant results were obtained using the Mann-Whitney test in the process of detecting changes in SSTs across the regions significantly correlated with the river streamflows across the Andes. In general higher SSTs during the interval 1975-1999 have been recorded in the Pacific, Atlantic and Indian Oceans, south of the Equator. Table 3 provides the Mann-Whitney test results applied to SSTs during different intervals. Changes detected in streamflow regimes (increase or decrease) and in SSTs (warming or cooling) are indicated in Table 4.

| River   | Region of the Ocean | N  | Neff | $r_c$ | $r_t$ | $\alpha(\%)$ | Figure |
|---------|---------------------|----|------|-------|-------|--------------|--------|
| Bermejo | Atlantic W          | 50 | 40   | 0.51  | 0.44  | 99.9         | 1.1    |
| Bermejo | Indian W            | 50 | 40   | 0.61  | 0.41  | 99.9         | 1.2    |
| Atuel   | Pacific SW          | 50 | 40   | -0.7  | 0.36  | 99.9         | 2.1    |
| Atuel   | Pacific SE          | 50 | 33   | 0.6   | 0.42  | 99.9         | 2.2    |
| Neuquén | Pacific SW          | 50 | 48   | -0.7  | 0.37  | 99.9         | 3      |
| Neuquén | Atlantic SW         | 50 | 49   | 0.52  | 0.44  | 99.9         | 3      |
| Neuquén | Tropical Pacific    | 50 | 49   | 0.39  | 0.36  | 99.0         | 3      |
| Limay   | Atlantic W          | 50 | 44   | -0.5  | 0.44  | 99.9         | 4.1    |
| Limay   | Pacific W           | 50 | 48   | -0.7  | 0.36  | 99.9         | 4.2    |
| Chubut  | Pacific S           | 50 | 46   | -0.5  | 0.44  | 99.9         | 5      |
| Chubut  | Tropical Atlantic   | 50 | 39   | -0.4  | 0.39  | 99.5         | 5      |

Table 2. Correlation coefficient between the SST from some selected sea areas and streamflows from the Andean rivers ( $r_c$ : correlation coefficient calculated,  $r_t$ : correlation coefficient tabulated,  $\alpha$ : Level of Significance).

| River   | $\alpha(\%)$ | Class. | Region of the Ocean identified | $\alpha(\%)$ | Class. |
|---------|--------------|--------|--------------------------------|--------------|--------|
| Bermejo | 99.9         | HS     | Atlantic W                     | 99.9         | HS     |
| Bermejo |              |        | Indian W                       | 99.9         | HS     |
| Atuel   | 99.0         | SD     | Pacific SE                     | 99.9         | HS     |
| Atuel   |              |        | Pacific SW                     | 95.0         | NSD    |
| Neuquén | 95.0         | NSD    | Pacific SW                     | 95.0         | NSD    |
| Neuquén |              |        | Atlantic SW                    | 95.0         | NSD    |
| Neuquén |              |        | Tropical Pacific               | 95.0         | NSD    |
| Limay   | 99.0         | SD     | Atlantic W                     | 99.0         | SD     |
| Limay   |              |        | Pacific W                      | 95.0         | MD     |
| Chubut  | 99.0         | SD     | Pacific S                      | 95.0         | NSD    |
| Chubut  |              |        | Tropical Atlantic              | 99.9         | HS     |

Table 3. Mann-Whitney Test for differences in mean populations between subperiods. Difference between intervals are classified as: HS: highly significantly; SD: significantly different; MD: marginally different; NSD not significantly different.

#### 4. CONCLUSIONS

As part of an integral project intended to analyze the impact of climatic changes on water resources across the Argentine Andean Cordillera, we identified in this study the ocean regions whose changes in temperature are strongly correlated with Andean river discharges. The influence of changes in SST over the climate of adjacent regions, and remote regions through teleconnections, has been largely acknowledged and our study provides additional evidence of these phenomena for the austral region of South America.

| River       | Observed Change | Region of the Ocean | Observed Change |
|-------------|-----------------|---------------------|-----------------|
| Bermejo (1) | Increase        | Atlantic W          | Warming         |
| Bermejo (1) |                 | Indian W            | Warming         |
| Atuel (1)   | Weak Increase   | Pacific SE          | Warming         |
| Atuel (1)   |                 | Pacific SW          | Weak Warming    |
| Neuquén (1) | Weak Decrease   | Pacific SW          | Not change      |
| Neuquén (1) |                 | Atlantic SW         | Weak Warming    |
| Neuquén (1) |                 | Tropical Pacific    | Weak Warming    |
| Limay (2)   | Decrease        | Atlantic W          | Warming         |
| Limay (2)   |                 | Pacific W           | Warming         |
| Chubut (2)  | Decrease        | Pacific S           | Not change      |
| Chubut (2)  |                 | Tropical Atlantic   | Warming         |

Table 4. Changes observed in mean streamflow and SST anomalies between the periods 1950-1974 and 1975-1999 (1), and between the periods 1950-1982 and 1983-1999 (2).

The spatial correlation patterns show geographical differences among the oceanic regions that influence changes in the discharges of rivers located in different sectors of the Andes: northwestern Argentina, the Central Andes of San Juan and Mendoza, and Northern Patagonia. The streamflow of Bermejo river, located north of 24°S, is strongly associated with temperatures in the subtropical Atlantic off the South American coast. These results are consistent with previous studies pointing at the subtropical Atlantic as one of the main sources of humidity for Northwestern Argentina (Barros et al. 2000; Vuille et al. 2004).

In response to the topography of the oceanic basins and the associated oceanic and atmospheric circulations, there are ocean regions where temperature evolves in a similar way. Recently, it has been observed that temperatures in the Subtropical Atlantic Ocean co-vary in a similar way with temperatures in the Subtropical Indian Ocean close to the African coast (Fauchereau et al., 2003). This can explain the significant correlations between the Bermejo river streamflow and the Subtropical Indian Ocean during the November-December period.

Relationships between precipitation in the Central Andes and Tropical Pacific SSTs have been observed by several researchers (Montecinos and Aceituno, 2003). In agreement with these observations, we found a strong relationship between variations in SST on the Tropical Pacific and the Atuel river streamflow. Relationships between SSTs and the discharge of rivers in the northern Patagonia are more difficult to interpret. It is quite probable that many of the observed spatial correlation patterns are owed to the way in which SSTs co-vary among different ocean regions. On the other hand, preliminary studies indicate that the Puelo river streamflow, on the western slope of the Patagonian Andes, is strongly regulated by changes in atmospheric circulation at high altitudes (Lara et al., submitted). In particular, a strong relationship between the Antarctic Oscillation (Gong, 1999) and the summer-fall Puelo river discharge has been observed. Unfortunately, our SST data set does not include records south of 45° S, hampering to identify the influence of high-latitude ocean circulation on the northern Patagonian (Limay and Chubut) river discharges.

In the mid 70's, a significant change was observed in the hydrologic regime of most rivers across the Andes with larger discharges for the rivers located in northwestern Argentina (Bermejo) but a reduction for the Patagonian (Limay and Chubut) rivers. Similar changes in SST anomalies were recorded in oceanic regions teleconnected with streamflow variations in many rivers along the Andes (Table 4). Some of the changes in streamflow during the past 50 years are related to warmer SST on the Pacific, Atlantic and Indian Oceans south of the Equator.

## 5. BIBLIOGRAPHY

Barros, V., Castañeda, M. E. y Doyle, M., 2000: Recent precipitation trends in southern South America east of the Andes: An indication of climatic variability. *Southern Hemisphere Paleo and Neo-Climates*, P. P. Smolka and W. Volkheimer, Eds., Springer-Verlag, 187–206.

Berri, G. J., Flamenco, E. A., Ghietto, M. A., Salazar, J. E., Sanchez, J., Portocarrero, C. A., 1997: The effect of ENSO on the river discharges of different hydrological systems in South America". Fifth International Conference on Southern Hemisphere Meteorology and Oceanography, Pretoria, South Africa.

Fauchereau, N., Trzaska, S., Richard, Y., Roucou, P. y Camberlin, P., 2003: Sea-Surface Temperature Co-Variability in the Southern Atlantic and Indian Oceans and its Connections with the atmospheric circulation in The Southern Hemisphere. *Int. J. Climatol.* **23**: 663–677.

Gong, D., Wang, S., 1999: Definition of Antarctic oscillation index. *Geophysical Research Letters*, 26, 4: 459-462.

Lara, A., Villalba, R. y Urrutia, R. submitted. A 400-year tree-ring record of the Río Puelo summer and early fall streamflow in the Valdivian rainforest Eco-region, Chile. *Climatic Change*.

Mechoso, C. R. y Iribarren, G. P., 1992 Streamflow in South America and the Southern Oscillation, *J. Climate*, 5, 1535-1539,1993.

Montecinos, A., y Aceituno, P., 2003: Seasonality of the ENSO-Related Rainfall Variability in Central Chile and Associated Circulation Anomalies. *Journal of Climate*, 16: 281-296.

Reynolds, R.W., and Smith, T.M., 1994: Improved global sea surface temperature analyses using optimum interpolation. *J. Climate*, 7, 929-948.

Slonosky, V. C., Jones, P. D., and Davies, T. D., 2000: Variability of the surface atmospheric circulation over Europe 1774-1995. *International Journal of Climatology*, 20, 1875-1897.

Tanco, R. A. y Berri, G. J., 2000: CLIMLAB2000, Version 1.1.0, A Statistical Software Package for Climate Applications. IRI-TR-00/1, International Research Institute (IRI) for Climate Prediction, LDEO, Palisades, N.Y., 10964 USA.

Valdés, J. B., Bastidas, L., Entekhabi, D., and García, N. , 1999: Climate-based Hydrologic Forecasting with Uncertainty Propagation. *24<sup>th</sup> Climate Diagnostic Workshop*, November 1-5, 1999, Tucson AZ.

Vuille, M., y Keimig, F. , 2004: Interannual Variability of Summertime Convective Cloudiness and Precipitation in the Central Andes Derived from ISCCP-B3 Data. *Journal of Climate*, 17: 3334-3348.